PHYSICAL REVIEW B **75**, 035403 (2007)

# Adsorption of methylamine on $\alpha$-$Al_2O_3$(0001) and $\alpha$-$Cr_2O_3$(0001): Density functional theory

Øyvind Borck,[1,2] Per Hyldgaard,[2,3] and Elsebeth Schröder[2]
[1]*Department of Physics, Norwegian University of Science and Technology, NO-7034 Trondheim, Norway*
[2]*Applied Physics, Chalmers University of Technology, SE-41296 Göteborg, Sweden*
[3]*Microtechnology and Nanoscience, Chalmers University of Technology, SE-41296 Göteborg, Sweden*

(Received 24 August 2006; revised manuscript received 9 November 2006; published 2 January 2007)

Using first-principles density functional theory calculations we analyze and compare molecular adsorption of methylamine ($CH_3NH_2$) at $\alpha$-$Al_2O_3$(0001) and $\alpha$-$Cr_2O_3$(0001). We report results for the adsorption structure and bonding nature as documented by the adsorption-induced changes in the electron density and in the projected density of states. We find that methylamine in both cases binds to exposed surface cations via the N lone-pair orbital. However, differences in the covalent bond affects the detail of the adsorption, surface relaxation, and electron transfer deep in the surfaces. We also find that an electrostatic bond between the amino-H and surface-O atoms supplements the N-cation bond for $\alpha$-$Cr_2O_3$(0001).

DOI: 10.1103/PhysRevB.75.035403 PACS number(s): 68.43.−h, 87.15.By, 68.47.Gh, 31.15.Ew

## I. INTRODUCTION

Adsorbing or grafting organic compounds on surfaces of oxides, metals, and semiconductors permits technological usage of the compounds as adhesives as well as protective and functional surface coatings. Organic compounds containing amino groups are used as glue, corrosion inhibitors, and for catalysis operation.[1,2] Adsorption of organic compounds, including DNA and polymers, on metallic nanoparticles is used for nanostructure functionalization. This is possible because the length of the molecules controls the nanoparticle organization[3] and because the presence of metallic nanoparticles modifies the polymer response.[4–6] Moreover, the successful grafting of molecular nanostructures on Si surfaces[7–11] could offer a more direct integration of organic-nanostructure devices with traditional semiconductor technology.

In this paper we use density functional theory (DFT) to characterize and compare the molecular adsorption of methylamine ($CH_3NH_2$) on alumina, $\alpha$-$Al_2O_3$(0001), and on chromia, $\alpha$-$Cr_2O_3$(0001). Supplementing also a previous comparison of methanol adsorption,[12,13] our study promotes the use of DFT as an independent tool for materials analysis of organic-compound coatings for aluminum-alloy surfaces.[2] The methylamine molecule is a natural test case for investigating the adhesion of amino-containing organics,[14,15] for example, amine-cured epoxy polymers. The naturally occurring aluminum-alloy surfaces sustain only a thin oxide film. Aluminum-alloy surfaces are often subject to a surface pretreatment prior to structural bonding or painting, with the aim of improving both the corrosion resistance and adhesive properties of the substrate.[2] This surface functionalization must be cost effective and avoid adverse environmental effects. Common pretreatments are anodizing and chromium-chromate conversion (CCC) coating. Essentially, anodizing is an electrochemical process which produces a thick aluminum-oxide film with greatly improved adhesive properties and corrosion resistance. Anodizing is extensively used by the aerospace industry to prepare the aluminum surface for painting and structural bonding.[2] The alternative CCC treatment results in the capping of the aluminum oxide by a chromium oxide surface layer (film). These CCC coatings provide excellent corrosion protection and adhesive properties, however, the presence of hexavalent chromium in the coating solution is a major health issue and has stimulated an active search for chromium-free alternatives. We seek to assist this search by developing insight on the nature of methylamine bonding on $\alpha$-$Al_2O_3$(0001) and $\alpha$-$Cr_2O_3$(0001), surfaces produced by the aluminum-alloy pretreatments.

DFT-based analysis and comparison of the molecular bonding provides details that are not otherwise available. Experimental results on methylamine adsorption on oxide surfaces are scarce[16] and do not reveal information on the interfacial structure and on the details of the bonding mechanisms. The adsorption of methylamine has been investigated experimentally on a range of transition-metal surfaces, including Cr,[17] Ni,[17] and Pd.[18] These studies indicate that methylamine binds to metal surfaces through lone-pair electrons on the nitrogen atom, and a corresponding mechanism is expected also for the metal-oxide surfaces.

*Ab initio* calculations permit a strategy where theory insight is sought to refine guidelines for surface functionalization. We present DFT calculations for methylamine adsorption at surfaces allowing for full relaxation of the atomic positions, extending a previous study of adsorption on $Cr_2O_3$ clusters.[14] We find that our DFT-based analysis of the adsorption-induced changes in the density and in the projected density of states reveal important insight on the nature of the bonding. We confirm that the adsorption involves bonding of the lone-pair electrons on the nitrogen atom to an exposed cation (metal) atom on the oxide surface. However, we also document clear differences in the covalent nature of this molecular bonding between the alumina and chromia adsorption cases. In addition, we find that an electrostatic interaction between the amino-H and surface-O supplements this covalent bonding in the case of chromia adsorption. By understanding the details in adsorption we refine the simpler picture of the adsorption and provide insight in terms of differentiation. This is important as it may allow us to ultimately suggest other, safer surface structures that mimic the bonding behavior (advantages) of $Cr_2O_3$(0001).

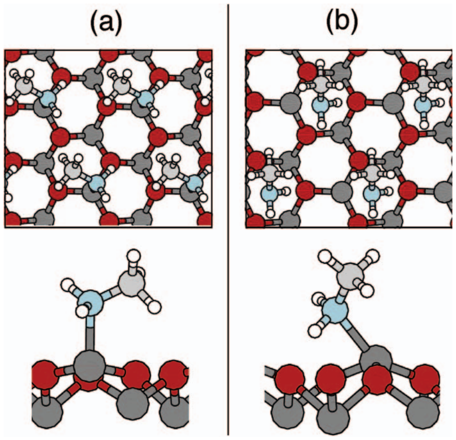

FIG. 1. (Color) Schematic side and top view of methylamine adsorbed at the (a) $\alpha$-$Al_2O_3$(0001) surface and (b) $\alpha$-$Cr_2O_3$(0001) surface in the 1 ML structures. The surface metal (oxygen) atoms are represented by dark gray (red) balls. Only the top layers of the slabs are shown.

## II. COMPUTATIONAL DETAILS

The calculations presented here are performed within the DFT approach using ultrasoft pseudopotentials[19] and a plane-wave basis set.[20] We use a 400 eV energy cutoff for the planewave expansion throughout our investigations. The exchange and correlation contributions to the total energy are approximated within the generalized gradient approximation (GGA), using the PW91 parametrization.[21] In our study of the isolated methylamine we use a fcc unit cell with lattice constant 12 Å, sampling the Brillouin zone only at the $\Gamma$ point. For the calculations of molecular adsorption on alumina and chromia we use a $4\times4\times1$ Monkhorst-Pack mesh.[22]

Figure 1 shows schematics of our two methylamine adsorption studies. We use slab models with periodic boundary conditions to describe the (0001) surfaces. Each slab consists of four M-$O_2$-M layers (M=Al, Cr), the periodic repetition of slabs are separated by ~15 Å of vacuum. We investigate the adsorption by placing molecules on one side of the slab only and we apply a dipole layer in the vacuum of the unit cell to exclude electrostatic effects.[23,24] The large separation (~5 Å) between active adsorption sites (outer-most metal atoms) makes it highly unlikely that the $Al_2O_3/Cr_2O_3$ surfaces support a dissociation-adsorption mechanism similar to those on the Si(001) surface.[9,11] In both corundum studies we use the Hellmann-Feynman forces to follow the atomic relaxation from a large number of initial molecular arrangements to determine the optimal adsorption configuration.

Our investigations of the adsorption on the $\alpha$-$Cr_2O_3$ ($\alpha$-$Al_2O_3$) surface are performed using spin-polarized calculations (spin-balanced calculations that assume an absence of spin polarization). In a pair of previous investigations[12,13] we have documented that our choice of convergence parameters produces an accurate description of both the bulk structure and pronounced atomic relaxations on the clean $\alpha$-$Al_2O_3$(0001) and $\alpha$-$Cr_2O_3$(0001) surfaces.[12,13] We also stress that the description accurately reproduces the antiferromagnetic distribution of atomic moments in bulk $\alpha$-$Cr_2O_3$.[13] We argue that the description therefore allows a detailed investigation and comparison of the nature of molecular bonding on the two corundum surfaces.

Adsorption of methylamine on $\alpha$-$Al_2O_3$ is considered both at coverage $\Theta=1/4$ monolayer (ML) and at coverage $\Theta=1$ ML in geometrical arrangements indicated in Fig. 1(a). In this definition of coverage, $\Theta=1$ ML corresponds to one adsorbed molecule per surface layer metal atom (that is, ~5 Å separation between the adsorbed methylamine molecules). Compared with the 1 ML coverage [Fig. 1(a)] there is no visible change in the atomic structure of methylamine at 1/4 ML. Adsorption of methylamine on $\alpha$-$Cr_2O_3$ is considered at coverage $\Theta=1$ ML. The spin-polarized nature makes investigations of the $\Theta=1/4$ ML $\alpha$-$Cr_2O_3$ adsorption intractable.

To investigate the nature of the molecule-surface bond we project the Kohn-Sham wavefunctions onto atomic orbitals to obtain the projected density of states (PDOS). To avoid double counting, we only consider the electron density inside projection spheres of radius 1 Å around each atom. We have checked that the choice of cutoff radius has no effect on the conclusions drawn from these plots.[25] To quantify the degree of ionicity in the bonding, i.e., the charge transfer, we employ Bader's "atoms-in-molecules" method[26] using the algorithm described in Ref. 27.

Our adsorption study does not include effects of oxygen defects in the oxide surfaces and focuses on perfect (and undoped) metal-oxide surfaces. The oxygen defects are expected to exist in most metal-oxide surfaces[28] and can provide active sites for the dissociation of molecules.[28,29] However, these effects are beyond the scope of this paper that investigates simple adsorption on the regular oxide surface. Nearby oxygen defects may still serve as charge traps that could modify the molecular adsorption on insulating surfaces in cases where the molecule-surface bond is predominantly ionic.[30] However, we find that the methylamine adsorption is predominantly covalent on $\alpha$-$Al_2O_3$(0001) and $\alpha$-$Cr_2O_3$(0001) and therefore expect the effects of oxygen defects to be minimal.

## III. RESULTS AND DISCUSSION

### A. The methylamine molecule

Table I summarizes our DFT results for the isolated methylamine molecule. This equilibrium structure agrees well with the experimental data.[31] The DFT results accurately reproduce the internal bond lengths and characteristic angles.

In Fig. 2 our corresponding DFT result for the highest-occupied molecular orbital (HOMO) of the methylamine molecule is shown. The plot illustrates the molecular structure, identifying the relaxed positions of the H atoms by the set of small balls, and those of C/N atoms by the topmost/lowest of the large balls. The plot also reports an isosurface plot of the HOMO wavefunction. We find that the HOMO of the methylamine molecule is a nonbonding lone-pair orbital dominated by the 2$p$ character of the nitrogen atom. The common view in chemical bonding theory is that the bonding at oxide surfaces results from a donation of methylamine

TABLE I. Comparison of the calculated and experimental geometry for the isolated methylamine molecule. Methylamine has a $C_s$ point group symmetry, possessing a mirror plane along the C-N bond that bisects the H-N-H plane. In the equilibrium, staggered conformation one methyl group hydrogen atom lies in the mirror plane at a distance $d_{\mathrm{CHip}}$ from the C atom, while the other two hydrogen atoms are out-of-plane at a distance of $d_{\mathrm{CHp}}$ from the C.

| | This work | Expt. (Ref. 31) |
|---|---|---|
| $d_{\mathrm{NH}}$ (Å) | 1.02 | 1.031 |
| $d_{\mathrm{CN}}$ (Å) | 1.46 | 1.472 |
| $d_{\mathrm{CHip}}$ (Å) | 1.11 | 1.112 |
| $d_{\mathrm{CHop}}$ (Å) | 1.10 | 1.112 |
| ∠CNH (°) | 112 | 111.5 |
| ∠HNH (°) | 107 | 106.0 |
| ∠HCH (°) | 107 | 108.4 |

lone-pair electron density to a partially empty cation orbital. This observation is used to guide our search for possible adsorption geometries below: we focus primarily on cases where the initial molecular arrangement has the nitrogen atom and its potentially reactive lone-pair orbital closest to the pair of corundum surfaces. However, we also include other molecular configurations in our search for the optimal adsorption configuration.

### B. Adsorption geometries and energetics

Table II and Fig. 1 summarize the main structural and energetic results of the present study. We comment on each of the adsorbate systems separately.

#### *1. Adsorption on* $\alpha$-$Al_2O_3$(0001)

Figure 1(a) shows the geometrical structure in the calculated optimal configuration for methylamine adsorption on $\alpha$-$Al_2O_3$(0001) at 1 ML coverage. The dark gray (red) balls identify the final, relaxed positions of the Al (O) atoms. This optimal adsorption structure is determined by following the atomic relaxation from a number of possible initial adsorption configurations at different high-symmetry sites at the $\alpha$-$Al_2O_3$(0001) surface. During the structure optimization we place no constraints on the motion of the molecule, so it is free to move laterally on (as well as perpendicularly to) the surface, and to reorient itself to locate the minimum energy adsorption structure.

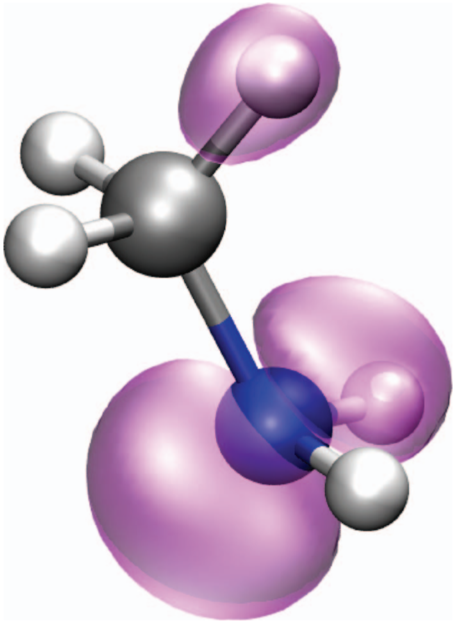

FIG. 2. (Color) The highest occupied molecular orbital of methylamine. The orbital is nonbonding with a predominant $2p$ character located at the N atom. Atom color coding as in Fig. 1.

Table II summarizes the optimal adsorption geometries that we calculate for both 1 ML and 1/4 ML coverage. We find that methylamine adsorbs with its N atom slightly laterally displaced from the Al on-top site by 0.36 Å in the case of 1 ML coverage and 0.15 Å in the case of 1/4 ML. The Al atom coordinated to methylamine experiences a very strong outward relaxation, as it is originally (in the clean surface) located below the outermost oxide layer.

We also determine the barrier for azimuthal rotation as less than 0.05 eV in the case of 1 ML coverage of methylamine adsorption on $\alpha$-$Al_2O_3$. The smallness of this barrier is in contrast to the large adsorption energies produced by the formation of a direct N-Al bond.

We stress that the optimal adsorption geometry contains no H-$O_{\mathrm{surf}}$ bonds for the $\alpha$-$Al_2O_3$ adsorption case. Such H-O bonds often form for molecular adsorption on oxide surfaces[12,32] and are also found for the methylamine on

TABLE II. Calculated adsorption energy and selected geometrical data for adsorption of methylamine on the (0001) surfaces of $\alpha$-$Al_2O_3$ and $\alpha$-$Cr_2O_3$. The distance $d_{\mathrm{MN}}$ is the nearest-neighbor separation between the N of $CH_3NH_2$ and a surface metal atom, $d_{\mathrm{HO}}$ is the shortest distance between a H atom of the amine group and a surface layer O atom. $h_{\mathrm{MO}}$ is the layer spacing between the metal atom to which the methylamine is bonded and the underlying O plane, with numbers in parentheses giving the differences compared to the clean surface. $\Phi$ is the tilt angle of the C-O bond with respect to the surface normal.

| | $\Theta$ (ML) | $E_{\mathrm{ads}}$ (eV) | $h_{\mathrm{MO}}$ (Å) | $d_{\mathrm{MN}}$ (Å) | $d_{\mathrm{CN}}$ (Å) | $d_{\mathrm{HO}}$ (Å) | $d_{\mathrm{NH1}}$ (Å) | $d_{\mathrm{NH2}}$ (Å) | ∠CNH1 (°) | ∠CNH2 (°) | $\Phi$ (°) |
|---|---|---|---|---|---|---|---|---|---|---|---|
| $\alpha-Al_2O_3$(0001) | | | | | | | | | | | |
| | 1/4 | 1.65 | 0.43(+0.32) | 1.98 | 1.48 | 2.99 | 1.03 | 1.03 | 111 | 111 | 60 |
| | 1 | 1.16 | 0.32(+0.21) | 2.05 | 1.46 | 2.11 | 1.02 | 1.05 | 113 | 112 | 49 |
| $\alpha-Cr_2O_3$(0001) | | | | | | | | | | | |
| | 1 | 0.80 | 0.56(+0.17) | 2.17 | 1.46 | 1.79 | 1.03 | 1.05 | 112 | 112 | 52 |

$\alpha$-$Cr_2O_3(0001)$ adsorption case. We have performed an extensive search for stable or even metastable configurations involving such H-O bonds on the $Al_2O_3$ surface. We have also documented that the adsorption configuration resembling the $Cr_2O_3$ adsorption problem is, in fact, directly unstable.

We note that the adsorption geometry of methylamine (Table II) shows no qualitative dependence on the coverage. Elastic deformations[33,34] and deformation energies play a significant but indirect role in determining the adsorption energy. However, it is clear that the coverage has almost no impact on the intramolecular arrangement. Instead the differences in the adsorption energies result from the elastic coupling mediated through the oxide surface, lowering of the adsorption energy with coverage (from 1.65 to 1.16 eV). The mechanism is similar to what we have previously discussed in a study of methanol adsorption.[12]

To test the observation directly, we also calculate the dependence of the adsorption energies with coverage on a pair of frozen surfaces. This study allows us, in part, to separate out the effects of electronic coupling which we find has a much smaller coverage dependence. Specifically, we find for the frozen-surface calculations that the adsorption energies only reduce from 1.11 eV at 1/4 ML to 0.94 eV at 1 ML coverage. The observation that the nature of bonding exhibits no dependence on coverage is confirmed by the analysis, below, in terms of the adsorption-induced changes to the electron density.

#### *2. Adsorption on* $\alpha$-$Cr_2O_3(0001)$

Figure 1(b) shows the final relaxed adsorption structure on the chromia surface. Again, the dark gray (red) balls represent the metal (oxygen) atoms. We find that methylamine on $\alpha$-$Cr_2O_3(0001)$ binds to a chromium atom but now with a different preferred lateral position for the N atom than on alumina. Rather than adsorbing on top of Cr, the molecule adsorbs with the N atom in a threefold hollow oxygen site [Fig. 1(b)]. A corresponding adsorption geometry on chromia has been documented for CO,[35] $H_2O$,[36] and methanol.[12]

Table II summarizes this optimal adsorption structure for methylamine on $\alpha$-$Cr_2O_3$ and allows a comparison with the above-presented results for $\alpha$-$Al_2O_3$. Similar to what we found for the $\alpha$-$Al_2O_3(0001)$ surface, the adsorption induces an outward relaxation of the Cr atom bound to the methylamine N. However, the relaxation is smaller as the Cr atom here originates from a position outside the oxygen atoms.[13] We find that the adsorption energy is weaker than in the aluminum oxide case, and is of the same size as the adsorption energy found in an earlier investigation[13] for methanol adsorbed at this surface.

### C. General discussion and nature of the methylamine bonding

To gain insight into the nature of the surface-molecular bond we compare the adsorption mechanisms at the $\alpha$-$Al_2O_3(0001)$ and $\alpha$-$Cr_2O_3(0001)$ surfaces. In this study we exploit the power of DFT to not only characterize the spatial variation of the bonding orbitals (Fig. 2) but also calculate the adsorption-induced differences in the electron density and in the orbital-projected density of states.

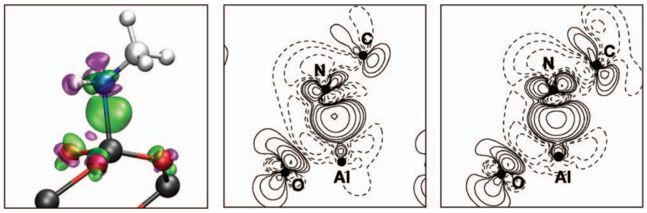

FIG. 3. (Color) Isosurface and contour variation in the adsorption-induced electron-density change for methylamine bonding on $\alpha$-$Al_2O_3(0001)$. Leftmost panel shows the isosurface variation with green (purple) regions identifying a gain (loss) of electron density. The middle and rightmost panels show contour plots of the electron density difference at 1 ML and 1/4 ML coverage, respectively. The contour plots are obtained in a plane through the C and N atoms of methylamine and a surface layer Al atom. Solid (dashed) lines indicate gain (loss) of electron density. The contours are drawn at densities $\Delta n = \pm 0.005 \times 2^k$ e/Å$^3$ for $k = 0,1,2,3,4,5$.

#### *1. Adsorption on* $\alpha$-$Al_2O_3(0001)$

Figure 3 reports our DFT results for the adsorption-induced differences in the electron density in the case of methylamine bonding on the $\alpha$-$Al_2O_3(0001)$ surface. We simply subtract the electron densities for the isolated molecule and surface (both with atoms fixed in the adsorption geometry) from the electron density that we calculate for the adsorbed system. The left panel shows the isosurface variation in the electron-density difference with areas of green (purple) shading indicating an electron gain (loss). The prominent feature of this figure is the increased density in the bonding region between N and Al. The loss of electron density appears to be largely from the N atom.

Our DFT calculations document that the methylamine adsorption is almost exclusively covalent in nature. The electron density buildup in the bonding region between N and Al is very much what one would expect for a covalent type of bonding.[37] To quantify the (lack of) ionicity in the molecular adsorption we perform a Bader analysis. While there are local charge-rearrangements, the overall charge transfer from the molecule to the surface is very small, and at the level of the computational uncertainty. We conclude that the nature of the bond therefore is close to purely covalent.

The middle and right panels of Fig. 3 show contour plots of the electron density difference in a plane containing the methylamine C and N atoms and a surface Al at coverages 1 ML and 1/4 ML, respectively. The shape of the electron density difference is very similar for these two coverages, suggesting that the bonding nature is similar. By comparing the contour plots in the middle and rightmost panels we conclude that the adsorption mechanism is only weakly dependent on the methylamine coverage. Some minor quantitative differences appear in the C-N bond region, however, it is evident in our comparison that the nature of bonding remains unchanged.

Important insight into the chemical bond formation can be extracted from such maps of the adsorption-induced differences in the electron density.[38] An electron buildup between

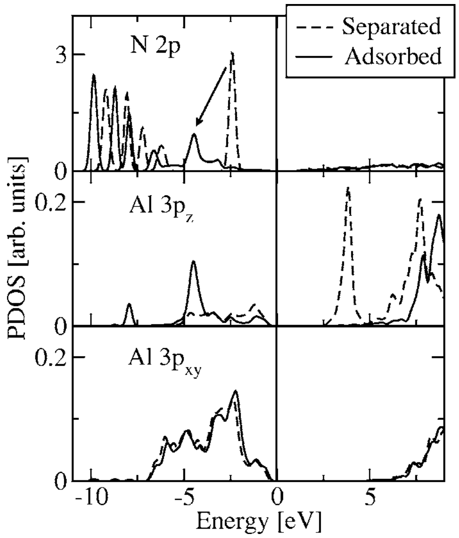

FIG. 4. Density of states projected onto the $p$ orbitals of N and surface layer Al for separated (noninteracting, ~4 Å above the surface) methylamine and $\alpha$-$Al_2O_3$(0001) compared to the adsorbate.

two atoms, as seen between the N and Al atom (Fig. 3), is a strong indication of a bond formation with a covalent character.

As mentioned above, the HOMO of methylamine is a nonbonding (lone-pair) orbital of predominantly N 2$p$ character (Fig. 2). The expectations from simple chemical bonding arguments is that bonding of the methylamine to an oxide surface is of a donor-acceptor character where the methylamine N lone-pair electron density "donates" electron density to a (partially) empty cation orbital.[28,39] This leads to a stabilization where, within a simplified one-electron picture, the (filled) lone-pair orbital moves down in energy, while the empty cation orbital acquires some antibonding character and is raised in energy.[28] A donor-acceptor interaction does not necessarily involve a charge transfer.

A comparison of Fig. 2 and Fig. 3 suggests that the lone-pair orbital of methylamine is involved in the methylamine-surface bonding. The PDOS shown in Fig. 4 confirms this expectation. The upper panel displays the density of states projected onto the N 2$p$ state. A comparison of the peaks corresponding to the free (dashed line) and adsorbed (solid line) molecule shows a general downshift in energy of the N 2$p$ states due to the adsorption. There is an additional downshift (stabilization) of the N 2$p$ state corresponding to the HOMO relative to the lower energy orbitals by ~2 eV, and also some broadening, indicating that mainly the lone-pair orbital is involved in the bonding of methylamine to the $\alpha$-$Al_2O_3$(0001) surface.

The middle and bottom panels of Fig. 4 display the density of states (DOS) projected onto the $3p_z$ and $3p_{xy}$ orbitals of the Al atom bound to the methylamine N. The $z$ axis is chosen to be parallel with the surface normal. As is evident from these plots, the Al $3p_{xy}$ state is affected very little by the adsorption, whereas the Al $3p_z$ state shows some small but important changes: The empty Al $3p_z$ band moves up in energy, and a peak appears in the valence band at the same energy as the HOMO N 2$p$ state. As mentioned above, the up-shift in energy of the empty cation states is expected from a donor-acceptor interaction. Furthermore, the changes to the valence band indicate some mixing of N 2$p$ and Al $3p_z$ states.

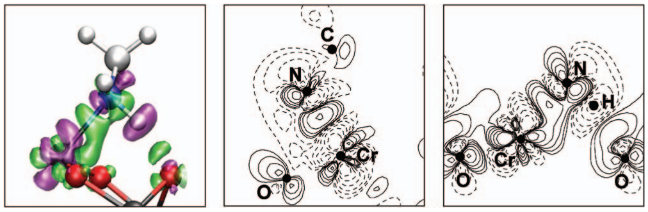

FIG. 5. (Color) Isosurface and contour variation in the adsorption-induced electron-density change for methylamine adsorption on $\alpha$-$Cr_2O_3$(0001). The leftmost panel shows the isosurface variation while the middle (rightmost) panel shows contour plots in the plane containing the bonding chromium atom and the molecule C and N (molecule N and the amine-group H) atoms. Coloring and contour lines as in Fig. 3.

Summarizing, our DFT calculations confirm the expectations from chemical bonding theory of a donor-acceptor interaction between the methylamine N lone-pair and an exposed surface (Al) cation. The bonding induces only a moderate orbital rearrangement and charge transfer within the $\alpha$-$Al_2O_3$(0001).

### *2. Adsorption on* $\alpha$-$Cr_2O_3$(0001)

Figure 5 shows our DFT results for the adsorption-induced changes in the electron density for the chromia surface. The most striking difference compared to adsorption on alumina is the more pronounced involvement of the cation ($d$-) states in the methylamine-chromia interactions.

As for the $Al_2O_3$, we find that the adsorption on $Cr_2O_3$ is almost purely covalent in nature. Again, the result of our DFT-based Bader analysis shows a negligible charge transfer. The differences in adsorption on $Al_2O_3$ and on $Cr_2O_3$ arise from differences in the details of the covalent bonding on the two surfaces.

The middle panel of Fig. 5 displays a contour plot of a cut in the electron density difference passing through the methylamine N and C atoms, and a surface Cr atom. The contour reveals an accumulation of electron density between the N and Cr atom as would also be expected for a covalent bonding of methylamine to the nearest-neighbor Cr atom via the N lone pair. In the rightmost panel, the methylamine N, one of the amine-group H atoms, and surface Cr and O atoms are intersected by the cut. A prominent feature in this contour plot is the loss of electron density around the H atom, and an increased electron density between the H atom and a surface O atom, indicating some H-O interaction in addition to the N-Cr interaction.

Comparing the adsorption-induced changes in electron density for the chromia and alumina adsorption systems we identify some differences which directly reflect the more pronounced covalent character of the bonding on chromia. Unlike in the alumina case, the charge buildup at the N-metal bond is compensated with finite intrasurface charge transfers also in the chromia surface layer. We stress that this en-

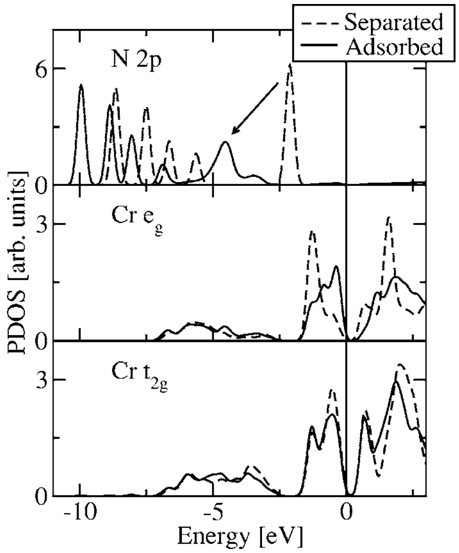

FIG. 6. Density of states projected onto the $p$ orbitals of N and onto the $d$ orbitals of the surface layer Cr for separated (noninteracting, ~4 Å above the surface) methylamine and $\alpha$-$Cr_2O_3(0001)$ compared to the adsorbate system.

hanced adsorption-induced hybridization with chromia surface levels is unlikely to arise from elastic effects because the chromia deformation is smaller than in the alumina adsorption case. Rather the increased hybridization throughout the surface region reflects a difference in the nature of the chemical bonding. This difference emphasizes that the methylamine adsorption on chromia cannot be viewed strictly within a simple electrostatic bonding model involving a coupling of the lone-pair electrons on the N atom to an exposed cation.

Figure 6 displays the DOS projected onto the N 2$p$ (upper panel), and Cr 3$d$ states (middle and lower panel). We adopt the notation used in investigations of the bulk electron structure.[40] In the middle panel we show the DOS projected onto the "$e_g$" orbitals (sum over $d_{xy}$, $d_{xz}$, and $d_{yz}$) and in the lower panel we show the "$t_{2g}$" orbitals (sum over $d_{z^2}$ and $d_{x^2-y^2}$) where the $z$ axis is chosen to be parallel with the surface normal. The "$t_{2g}$"-like states (Fig. 6, bottom panel) only show a small perturbation as result of the adsorption. The "$e_g$"-like orbitals, however, show some shift toward higher energy, this can be interpreted as due to a donor-acceptor interaction with the methylamine N "lone pair."

Comparing the adsorption-induced changes in the projected density of states for the chromia and alumina systems reveals differences in the covalent nature of the bonding. The adsorption-induced changes to the N 2$p$ state are somewhat similar to those of the alumina case. Specifically, a similar stabilization of the HOMO level arises with the adsorption but the effect is more pronounced in the chromia case (~2.4 eV as opposed to ~2.1 eV on alumina). The broadening is also larger for chromia, reflecting the larger ability (Fig. 5) to hybridize with the states in the chromia surface layer. The adsorption at the chromia surface is dominated by the d-band interaction, less electrostatic in nature, and too complex to be fully discussed as a lone-pair interaction with the exposed cation.

## IV. CONCLUSIONS

We find that methylamine adsorbs strongly to both the $\alpha$-$Al_2O_3(0001)$ and the $\alpha$-$Cr_2O_3(0001)$ by the amino group and onto an exposed surface layer cation atom. We also find that adsorption induces strong relaxation of the surface structure and is associated by large elastic deformations and deformations energies. We have analyzed and compared the nature of bonding by studying the adsorption-induced changes in both the electron density and in the projected density of states. Our analysis confirms expectations from chemical bonding theory of a donor-acceptor interaction involving a lone-pair on the methylamine N atom and an exposed surface cation. At the same time we also find marked differences between the adsorption cases. These differences are ascribed to the covalent bonding as revealed by our DFT-based analysis of the adsorption-induced changes in the density and in the projected density of states. Our investigations show that DFT provides the characterization needed to extend the simple chemical bonding theory and insight which is needed to begin a wider search for grafting organic compounds, for example, on pretreated aluminum-alloy surfaces.

## ACKNOWLEDGMENTS

This work was partly carried out within *Light Metal Surface Science*, a joint project between SINTEF and NTNU, financed by The Norwegian Research Council (NFR), Hydro Aluminium, Profillakkering AS, Norsk Industrilakkering AS, Fundamus AS, Jotun Powder Coatings AS, and DuPont Powder Coating. NFR and NTNU are acknowledged for support through computing time at the Norwegian High Performance Computing Center (NOTUR). The work of E.S. and P.H. was supported by the Swedish Research Council (VR) and by the Swedish Foundation for Strategic Research (SSF) through the consortium ATOMICS.

---

[1] S. A. Lawrence, *Amines: Synthesis, Properties and Applications* (Cambridge University Press, Cambridge, 2004).

[2] M. M. Hyland, in *Handbook of Aluminum. Volume 2: Alloy Production and Materials Manufacturing*, edited by G. E. Totten and D. S. MacKenzie (Marcel Dekker, New York, 2003).

[3] Z. Gueroui and A. Libchaber, Phys. Rev. Lett. **93**, 166108 (2004).

[4] B. Dubertret, M. Calame, and A. J. Libchaber, Nat. Biotechnol. **19**, 365 (2001).

[5] W. Fritzsche and T. A. Taton, Nanotechnology **14**, R63 (2003).

[6] B.-K. Pong, J.-Y. Lee, and B. L. Trout, Langmuir **21**, 11599 (2005).

[7] R. J. Hamers, J. S. Hovis, S. Lee, H. Liu, and J. Shan, J. Phys. Chem. **101**, 1089 (1996).

[8] G. P. Lopinski, D. D. M. Wayner, and R. A. Wolkow, Nature (London) **406**, 48 (2000).

[9] K. T. Queeney, Y. J. Chabal, and K. Raghavachari, Phys. Rev. Lett. **86**, 1046 (2001).

[10] C. Mui, G. T. Wang, S. F. Bent, and C. B. Musgrave, J. Chem. Phys. **114**, 10170 (2001).

[11] J.-H. Cho and L. Kleinman, Phys. Rev. B **67**, 201301(R) (2003).

[12] Ø. Borck and E. Schröder, J. Phys.: Condens. Matter **18**, 1 (2006).

[13] Ø. Borck and E. Schröder, J. Phys.: Condens. Matter **18**, 10751 (2006).

[14] C. Compere, D. Costa, L.-H. Jolly, E. Mauger, and C. Giessner-Prettre, New J. Chem. **24**, 993 (2000).

[15] S. Yanagisawa, T. Tsuneda, K. Hirao, and Y. Matsuzaki, THEOCHEM **716**, 45 (2005).

[16] L.-F. Liao, W.-C. Wu, C.-C. Chuang, and J.-L. Lin, J. Phys. Chem. B **105**, 5928 (2001).

[17] A. G. Baca, M. A. Schultz, and D. A. Shirley, J. Chem. Phys. **83**, 6001 (1985).

[18] J. J. Chen and N. Winograd, Surf. Sci. **326**, 285 (1995), and references therein.

[19] D. Vanderbilt, Phys. Rev. B **41**, 7892 (1990).

[20] The DACAPO code can be downloaded from http://wiki.fysik.dtu.dk/dacapo

[21] J. P. Perdew, J. A. Chevary, S. H. Vosko, K. A. Jackson, M. R. Pederson, D. J. Singh, and C. Fiolhais, Phys. Rev. B **46**, 6671 (1992); **48**, 4978(E) (1993).

[22] H. J. Monkhorst and J. D. Pack, Phys. Rev. B **13**, 5188 (1976).

[23] J. Neugebauer and M. Scheffler, Phys. Rev. B **46**, 16067 (1992).

[24] L. Bengtsson, Phys. Rev. B **59**, (1999) 12301.

[25] The PDOS provides valuable qualitative information even if there is no natural definition of the projection sphere cutoff radius $r_c$. From the Bader analysis it is possible to define a physically motivated choice of $r_c$ (designed to enclose the same amount of charge as the Bader volume). A safe choice is $r_c=1$ Å, that prevents any overlap in the atomic projection. We find no qualitative differences in the PDOS obtained with these two values of $r_c$.

[26] R. F. W. Bader, *Atoms in Molecules—A Quantum Theory* (Oxford University Press, Oxford, 1990).

[27] G. Henkelman, A. Arnaldsson, and H. Jónsson, Comput. Mater. Sci. **36**, 254 (2006).

[28] V. E. Henrich and P. A. Cox, *The Surface Science of Metal Oxides* (Cambridge University Press, Oxford, 1994).

[29] R. Schaub, P. Thostrup, N. Lopez, E. Lægsgaard, I. Stensgaard, J. K. Nørskov, and F. Besenbacher, Phys. Rev. Lett. **87**, 266104 (2001).

[30] G. Pacchioni, ChemPhysChem **4**, 1041 (2003).

[31] T. Iijima, H. Jimbo, and M. Taguchi, J. Mol. Struct. **144**, 381 (1986).

[32] H. E. Sanders, P. Gardner, and D. A. King, Surf. Sci. **331**, 1496 (1995).

[33] K. H. Lau and W. Kohn, Surf. Sci. **65**, 607 (1977).

[34] K. H. Lau and W. Kohn, Surf. Sci. **75**, 69 (1978).

[35] M. Pykavy, V. Staemmler, O. Seiferth, and H.-J. Freund, Surf. Sci. **479**, 11 (2001).

[36] T. Bredow, Surf. Sci. **401**, 82 (1998).

[37] P. Coppens, *X-Ray Charge Densities and Chemical Bonding* (Oxford University Press, Oxford, 1997).

[38] V. G. Tsirelson and R. P. Ozerov, *Electron Density and Bonding in Crystals* (IOP, Bristol, 1996).

[39] R. Hoffmann, Rev. Mod. Phys. **60**, 601 (1988).

[40] P. A. Cox, *Transition Metal Oxides: An Introduction to their Electronic Structure and Properties* (Clarendon, Oxford, 1992).